PHYSICAL REVIEW B VOLUME 26, NUMBER 4 15 AUGUST 1982

Quasi-two-dimensional photoexcited carriers in GaAs doping superlattices

Ch. Zeller, B. Vinter, and G. Abstreiter
Physik-Department, Technische Universität München, D-8046 Garching, Federal Republic of Germany

K. Ploog
Max-Planck-Institut für Festkörperforschung, D-7000 Stuttgart 80, Federal Republic of Germany
(Received 30 March 1982)

Periodic multilayer structures of GaAs exhibit new semiconductor properties such as tunable effective band gap, long lifetime of photoexcited carriers, and quantization of carriers in space-charge-induced potential wells. We present a more careful treatment of the high excitation regime, where the subbands broaden into minibands, than earlier self-consistent calculations. Experimentally we have used photoluminescence and resonant inelastic light scattering measurements to study the subband structure. The luminescence peak is found to shift with decreasing photoexcitation intensity far below the band gap of GaAs. By comparing the peak position with the theory we determine the carrier concentration. Resonant spin-flip single-particle excitations directly give the subband splittings which are in good agreement with the theoretical results. At high excitation intensities, the subbands merge and a quasi-three-dimensional behavior is found.

I. INTRODUCTION

In recent years extensive theoretical and experimental studies of artificial semiconductor superlattices have been performed. Most of the work was focused on the electrical and optical properties of the compositional multilayer structures $Al_xGa_{1-x}As$-GaAs (Ref. 1) and InAs-GaSb (Ref. 2). The introduction of the modulation-doping technique[3] has opened new possibilities, especially in connection with the strongly enhanced mobilities[4] of transferred electrons in such structures. The progress achieved is due to the further development of molecular-beam epitaxy as an excellent crystal-growth technique used for the preparation of ultrathin semiconducting films of different composition and/or doping.

Apart from these successful achievements in the field of compositional multi-quantum well structures, extensive theoretical studies of a different type of artificial semiconductor superlattice composed of ultrathin n- and p-doped semiconductor layers have been performed already by Döhler ten years ago.[5] More recently,[6] Döhler has shown that these new types of superlattices should have a number of new properties such as tunable effective band gap, long lifetime of photoexcited carriers, quantization of carriers in space-charge induced-potential wells, and tunable absorption coefficients. The development of abrupt doping techniques in combination with molecular-beam epitaxy recently made feasible the growth of GaAs-doping superlattices.[7] In these so-called n-i-p-i crystals the electrons of the donor impurities in the n-type layers are transferred in space to the acceptor sites in the p-type layers. This results in space-charge potentials perpendicular to the layers caused by the ionized impurities. It is easy to calculate the space-charge potential and the subband splitting in this situation. The potential-well depth and the subband energies depend only on the layer thickness d_n and d_p and on the impurity concentration N_D and N_A.

The first experimental evidence for the validity of the basic theoretical ideas was the observation of strong-absorption tails extending far into the gap of the pure material.[7] The direct observation of a tunable effective band gap and the quantization of photoexcited carriers in space-charge potential wells has been reported recently.[8]

In this work we present more extensive studies of both photoluminescence and resonant inelastic light scattering experiments of different GaAs-doping superlattice structures. In Sec. II we discuss the concept and theoretical calculations of subband energies in such n-i-p-i crystals. We treat more carefully than previous calculations[8] the highly excited regime where effects associated with

the finite-miniband width of the subbands became noticeable. In Sec. III the sample characterization and the experimental techniques are described. The experimental results are discussed in Sec. IV followed by some concluding remarks.

II. MINIBAND THEORY

The theory of the electronic structure of *n-i-p-i* superlattices has been developed by Döhler[5,6] and by Döhler and co-workers.[8–10] When the superlattice potential is deep, the electrons are strongly bound to one layer and the superlattice potential can be treated as a series of independent potential wells in which the electrons behave quasi-two-dimensionally. It is well known that the binding of the electrons leads to quantization into subbands with dispersion,

$$\epsilon_n(\vec{k}_{||})=E_n+\frac{\hbar^2 k_{||}^2}{2m} , \tag{1}$$

where $\vec{k}_{||}$ is the wave vector parallel to the layers, m is the electron effective mass, and the subband bottom energies E_n are eigenvalues of the one-dimensional Schrödinger equation

$$-\frac{\hbar^2}{2m}\frac{d^2}{dz^2}\xi_n(z)+V(z)\xi_n(z)=E_n\xi_n(z) , \tag{2}$$

where $V(z)$ is the superlattice potential in one layer. The potential consists of the potential from ionized impurities and of the direct Hartree potential from the electrons themselves. Inclusion of exchange and correlation effects through the local-density-functional formalism does not change the results much.[10] It was shown in Ref. 8 that the calculated subband-energy separations agree well with resonant Raman scattering measurements.

In this work we present a more careful treatment of the highly excited case in which so many electrons are created that states with energy near or even above the top of the superlattice potentials are occupied. In that case the two-dimensional nature of the system is less pronounced, since electrons can easily tunnel between the wells. We mention that for the $Al_xGa_{1-x}As$-GaAs superlattice such states have been investigated by Ando and Mori.[11] Our method of solution is quite different from theirs, however, so we describe it in some detail here.

The potential $V(z)$ is a periodic function of z, $V(z+d)=V(z)$, $-\infty<z<\infty$, where $d=d_n+d_p$ is the superlattice period, and we chose $z=0$ in the middle of an n-type layer so that the potential is also even $V(z)=V(-z)$. For such a potential the stationary states are a product of plane waves parallel and Bloch waves perpendicular to the layers. The Bloch waves $\psi_{nk}(z)$ have the form

$$\psi_{nk}(z)=u_{nk}(z)e^{ikz} , \tag{3}$$

where n is a miniband index, k a wave vector in the first Brillouin zone

$$-\frac{\pi}{d}<k<\frac{\pi}{d} ,$$

and $u_{nk}(z)$ is periodic

$$u_{nk}(z)=u_{nk}(z+d) .$$

The Bloch function satisfies the Schrödinger equation

$$\left[-\frac{\hbar^2}{2m}\frac{d^2}{dz^2}+V(z)\right]\psi_{nk}(z)=E_n(k)\psi_{nk}(z) . \tag{4}$$

Instead of solving this eigenvalue equation for a given k we go the opposite way and choose the energy E. By direct integration starting from $z=0$ we construct two real solutions, $\psi_1(z)$ and $\psi_2(z)$, to the Schrödinger equation in the interval

$$-\frac{d}{2}<z<\frac{d}{2} .$$

We choose initial conditions $\psi_1(0)=0,\psi_1'(0)=1$ and $\psi_2(0)=1,\psi_2'(0)=0$.

Because of symmetry around $z=0$ we have

$$\psi_1(z)=-\psi_1(-z)$$

and

$$\psi_2(z)=\psi_2(-z) ,$$

so at the end points we have

$$\begin{aligned} p_1&\equiv\psi_1\left[\frac{d}{2}\right]=-\psi_1\left[-\frac{d}{2}\right] ,\\ p_1'&\equiv\psi_1'\left[\frac{d}{2}\right]=\psi_1'\left[-\frac{d}{2}\right] ,\\ p_2&\equiv\psi_2\left[\frac{d}{2}\right]=\psi_2\left[-\frac{d}{2}\right] ,\\ p_2'&\equiv\psi_2'\left[\frac{d}{2}\right]=-\psi_2'\left[-\frac{d}{2}\right] . \end{aligned} \tag{5}$$

We then try to find a Bloch solution as a linear combination of these two solutions:

$$u_{nk}(z)e^{ikz}=a_1\psi_1(z)+a_2\psi_2(z) . \tag{6}$$

The periodicity of $u_{nk}(z)$ applied at $\pm d/2$ leads to

a homogeneous system of linear equations for a_1 and a_2,

$$p_1(1+e^{ikd})a_1+p_2(1-e^{ikd})a_2=0\,,$$
$$p_1'(1-e^{ikd})a_1+p_2'(1+e^{ikd})a_2=0\,, \tag{7}$$

which has a nonzero solution only if

$$e^{2ikd}-e^{ikd}(p_1p_2'+p_2p_1')+1=0\,, \tag{8}$$

where we have made use of the fact that the Wronskian

$$\psi_1(z)\psi_2'(z)-\psi_2(z)\psi_1'(z)=-1\,.$$

For $|p_1p_2'+p_2p_1'|>2$ this equation has purely imaginary solutions for k, so that the chosen energy lies in a gap. For

$$|p_1p_2'+p_2p_1'|\leq 2$$

we have two symmetric real k values in the first Brillouin zone, and from Eqs. (6) and (7) we can find the corresponding two Bloch solutions $u_{nk}e^{ikz}$ and $u_{n_1-k}e^{-ikz}$.

If we normalize so that

$$\int_{-d/2}^{d/2}|u_{nk}(z)|^2dz=1\,, \tag{9}$$

the electron density is given by (for temperature $T=0$ K)

$$\rho(z)=\frac{md}{\pi\hbar^2}\sum_n\int_{-\pi/d}^{\pi/d}\frac{dk}{2\pi}[E_F-E_n(k)]\Theta(E_F-E_n(k))\,|u_{nk}(z)|^2\,, \tag{10}$$

where the Fermi energy E_F is determined by the condition

$$N=\frac{md}{\pi\hbar^2}\sum_n\int_{-\pi/d}^{\pi/d}\frac{dk}{2\pi}[E_F-E_n(k)]\Theta(E_F-E_n(k))\,, \tag{11}$$

and N is the areal density of electrons per lattice period.

Having shown how we solve the Schrödinger equation (4), we make the Hartree approximation in the standard way, i.e., the lattice potential is determined by solving Poisson's equation

$$\frac{d^2V}{dz^2}=-\frac{e^2}{\epsilon}[\rho(z)-N_D(z)+N_A(z)]\,, \tag{12}$$

where $N_D(z)$ and $N_A(z)$ are the distributions of ionized donors and acceptors and ϵ is the permittivity of GaAs. The Poisson and the Schrödinger equations are calculated self-consistently. Because of macroscopic charge neutrality, acceptors in a sufficiently broad region around the top of the potential well will be neutralized to compensate for the charge of the free electrons. The charge-neutrality condition and symmetry secure that the whole periodic lattice potential can be found by integrating Poisson's equation in one lattice period with the initial condition $dV/dz=0$ for $z=0$. Compared with the method of Ando and Mori[11] the advantages of this method are that all calculations are done in one well and that diagonalization of matrices of high rank is avoided.

It should be mentioned that in practice we first determine the miniband edges $E_n(k=0)$ and $E_n(k=\pi/d)$ by iteration. $\epsilon=12.53\epsilon_0$ and $m=0.067m_0$ have been used in the calculations.

In Fig. 1 we show some characteristic results in a highly excited case. Contrary to the weakly excited case, where the potential well is almost parabolic and the subbands almost equidistant, we have here a much shallower and more rectangular potential. Consequently, the subband separation between the lowest two subbands is smaller than be-

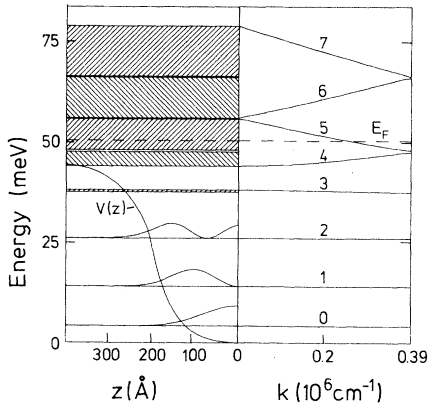

FIG. 1. Results of theoretical calculations for a sample with $d_n=d_p=40$ nm and $N_D=N_A=10^{18}$ cm^{-3} in a highly excited case with a two-dimensional concentration of 3.75×10^{12} cm^{-2}. Left side: self-consistent potential $V(z)$ and energy levels. The square of the electron wave function is shown for the lowest three subbands. The widths of the minibands are indicated by hatches. Right side: dispersion $E_n(k)$ in the direction perpendicular to the layers.

tween the next two subbands. Near the top of the potential the wave function between neighboring wells overlaps strongly and therefore the subbands broaden to minibands with considerable dispersion in $E_n(k)$ shown in the right part of the figure. For energies sufficiently high above the top of the potential the gaps become small and the electrons are almost free in the direction perpendicular to the superlattice layers also, so that we have a three-dimensional almost-free-electron gas. The results of this theory are compared with the experiments described in Sec. IV.

III. EXPERIMENTAL TECHNIQUES

The GaAs *n-i-p-i* structures used in the present experiments have been prepared by molecular-beam epitaxy. Twenty alternative *n*(Si)- and *p*(Be)-doped GaAs layers were grown on a semi-insulating or n^+-GaAs (100) substrate. The doping concentration $N_D=N_A=1\times10^{18}$ cm^{-3} was the same for all layers. The individual layer thickness (d_n and d_p) varies from 20 nm in sample 2227 to 60 nm in sample 2229. In the ground state we have $N_D d_n = N_A d_p$ which is the situation of the compensated *n-i-p-i* crystal. The ground-state parameters of the samples studied are summarized in Table I.

In the ground state the periodic potential well is parabolic, which results in an equidistant spacing of the subbands. The effective-energy gap E_g^{eff}, approximately given by E_g-2V_0 with $E_g\simeq1.52$ eV, is the low-energy limit of the tunability of the optical properties of these structures.

In *n-i-p-i* crystals photoexcited electron-hole pairs are separated in space and collected in the respective doped layers. The Hartree potential of free carriers is then added to the space-charge potential of the ionized impurities which results in an increased effective-energy gap E_g^{eff} and, consequently, in a decreased well depth and subband splitting. In order to study these effects, we have performed photoluminescence and inelastic light scattering experiments as shown schematically in Fig. 2. The samples were mounted in the exchange gas chamber of a temperature-variable cryostat and cooled to $T\simeq10$ K. The photoexcitation was produced by the 647.1-nm emission line of the Kr^+ ion laser. The power density was varied by several orders of magnitude using attenuators and point and line focus. The backscattered light was collected and focused on the entrance slit of a Jarrel-Ash double monochromator and analyzed and detected with a GaAs photomultiplier tube and conventional pulse-counting electronics. In the used setup spectra could be obtained down to 1.35 eV where both our spectrometer and the photomultiplier have their cutoff.

TABLE I. Parameters of the studied *n-i-p-i* crystals in the ground state. $2V_0$ is the depth of the potential wells.

Sample	$d_n=d_p$ (nm)	$N_D=N_A$ (cm^{-3})	$2V_0$ (meV)	$N_D d_n$ (cm^{-2})
2227	20	1×10^{18}	144	2×10^{12}
2228	40	1×10^{18}	578	4×10^{12}
2229	60	1×10^{18}	1300	6×10^{12}

IV. RESULTS AND DISCUSSIONS

In order to obtain information on the tunability of the effective energy gap and on the photoexcited quasistable carrier concentration per layer, we have studied the photoluminescence spectra of the three samples using different excitation intensities. The luminescence in excited GaAs-doping superlattices arises from the recombination of electrons in the occupied subbands with the holes which are assumed to occupy a narrow impurity band centered around the position of the acceptor levels in the *p*-type layers. This assumption is reasonable in view of the large difference of the effective mass of holes and electrons. Also we find experimentally

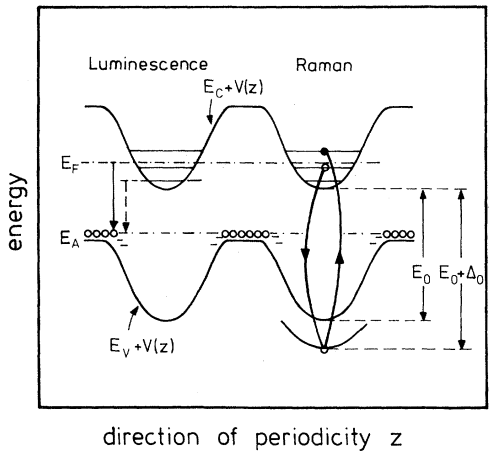

FIG. 2. Real-space energy diagram of an excited *n-i-p-i* crystal. E_c and E_v are the conduction- and valence-band edges, respectively, E_F is the Fermi energy in the conduction band, E_A is the acceptor level, and $V(z)$ is the superlattice potential. The Raman and luminescence processes are shown schematically.

that in homogeneously doped p-type GaAs (Be) the low temperature luminescence remains relatively sharp up to concentrations of 1×10^{19} cm^{-3} and is mainly due to transitions from the conduction band to the Be-acceptor levels.[12] In homogeneously doped n-type GaAs (Si), on the other hand, the system is already degenerate at donor concentrations $N_D \gtrsim 1\times10^{17}$ cm^{-3}.

In n-i-p-i crystals the excited electrons and holes are separated in space. The recombination is due to the overlap of the wave functions of the electrons in the subbands or minibands with the acceptor-band wave functions. At low excitation intensities, this overlap is extremely small. However, it increases exponentially with increasing carrier concentration. In addition, the strongest overlap occurs for the highest occupied subband. In the quasi-two-dimensional case the density of states is constant in each subband. Consequently, we expect a staircaselike luminescence line shape with the high energy onset at E_F-E_A, where E_F is the Fermi energy in the conduction band and E_A is the energy of the acceptor impurity band. As discussed already in Ref. 8, the steplike character of the luminescence has not been observed, which is caused by the inhomogeneous excitation of the individual layers due to the limited penetration depth of the laser light.

In Fig. 3 we show some photoluminescence spectra of sample 2227 obtained with different excitation intensities. The observed peaks are asymmetric with a relatively sharp onset on the high-energy side and a tail on the low-energy side. The peak position shifts to higher energies with increasing excitation intensity. At very high laser excitation the peak approaches the band gap of GaAs and the line is more symmetric. Similar results have been obtained for the other samples. The red shift of the luminescence peak for low-excitation intensities is much stronger in the n-i-p-i crystals 2228 and 2229 which have a larger width of the layers and, consequently, much deeper potential wells at a fixed carrier concentration.

On the left-hand side of Fig. 4 we show the shift of the luminescence peak for the three samples versus excitation intensity. The experimental points mark the inflection points on the high-energy side of the luminescence lines. These values correspond to the energy difference E_F-E_A. Using the calculations described in Sec. II, we can now convert the laser-excitation scale to a carrier-density scale N per layer. The theoretical results for E_F-E_A for the three samples are shown on the right-hand side of Fig. 4. This figure is used to

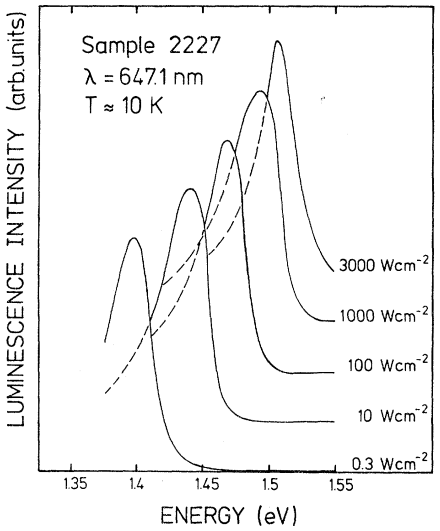

FIG. 3. Photoluminescence spectra of a GaAs n-i-p-i superlattice with $d_n=d_p=20$ nm and $N_A=N_D=10^{18}$ cm^{-3} at different laser-excitation intensities.

determine the two-dimensional carrier concentration from the luminescence peaks. It should be mentioned that at very high excitation intensities, when the lines are more symmetric and approach the GaAs energy gap, this method gives only a lower limit of N.

In order to get direct information on the subband splitting, we have performed resonant inelastic light scattering experiments. This technique has been successfully applied to study the subband splitting of two-dimensional electron systems in $Al_xGa_{1-x}As$-GaAs single heterojunctions[13] and multiquantum well structures.[14] The relevant light scattering processes in two-dimensional plasmas have been discussed theoretically by Burstein *et al.*[15] based on the theory of light scattering by three-dimensional carrier systems. There have also been some successful attempts made to observe light scattering by photoexcited carriers in undoped quantum well structures,[16] as well as in pure, homogeneous GaAs.[17,18] Compared with n-i-p-i crystals, however, the situation there is different because the electron-hole pairs are not separated in space. Consequently, their recombination lifetime is much shorter. The photoexcited plasma in a homogeneously doped or pure semiconductor is a multicomponent carrier system which gives rise to acoustic-plasma modes which have been observed recently.[18]

To observe light scattering signals of a quasi-two-dimensional electron system it is necessary to work under resonance conditions where the scatter-

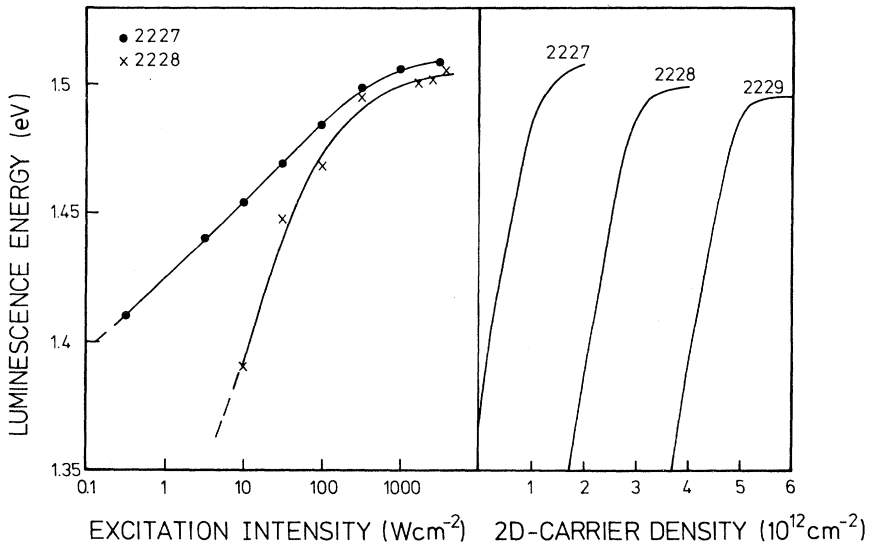

FIG. 4. Left side: measured high-energy cutoff of photoluminescence as a function of excitation intensity for the samples 2227 and 2228. The behavior of sample 2229 is similar to that of sample 2228. Right side: theoretical dependence of $E_F - E_A$ on the two-dimensional carrier density.

ing cross-section is strongly enhanced. The 647.1-nm laser line used in our experiments is close to the $E_0+\Delta_0$ gap of GaAs. At this energy gap the resonance condition is only fulfilled for electrons in the conduction band, but not for holes in the valence band. It has been shown that at this resonance both the spin-flip single particle and the collective excitations of the carrier system can be observed. Spin-flip single-particle excitations give direct information on the subband splitting, while the collective excitations have been used to study the depolarization shift and the Coulomb matrix elements in $Al_xGa_{1-x}As$-GaAs multiquantum well structures.[19,20]

In Ref. 8 it was shown that spin-flip single-particle excitations can be used to study subband splittings in *n-i-p-i* crystals. The scattering process is shown schematically in Fig. 2. For the Raman experiments the inhomogeneous excitation due to the limited penetration depth of the incident laser light is not so important as for luminescence experiments for two reasons: (i) the subband splitting is less sensitive to the excitation intensity than the effective-energy gap, (ii) the scattered light is strongly reabsorbed, and consequently, signals from the constituent *n-i-p-i* layers close to the surface are heavily weighted in the spectra.

In Figs. 5–7 we show the experimental results for the three studied *n-i-p-i* crystals. Spectra are shown for several excitation intensities. The dashed lines indicate the $E_0+\Delta_0$ hot-luminescence background which is always observed in *n* GaAs. On top of this background distinct peaks are seen (marked by the arrows). In all samples these peaks shift to smaller energies with increasing excitation

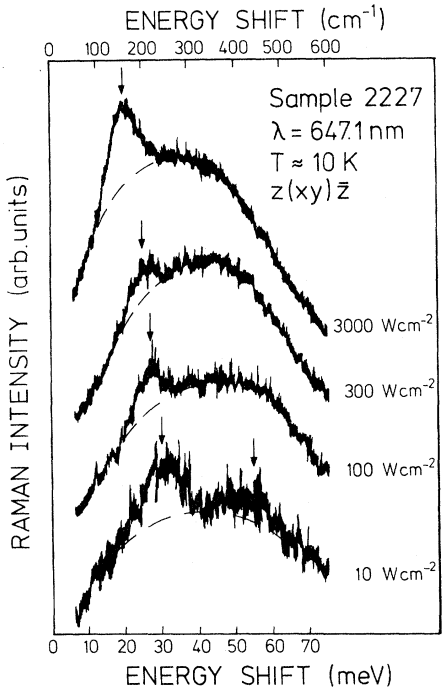

FIG. 5. Single-particle light scattering spectra at different excitation intensities. The subband transitions are marked by arrows. The dashed lines indicate the $E_0+\Delta_0$ hot-luminescence background.

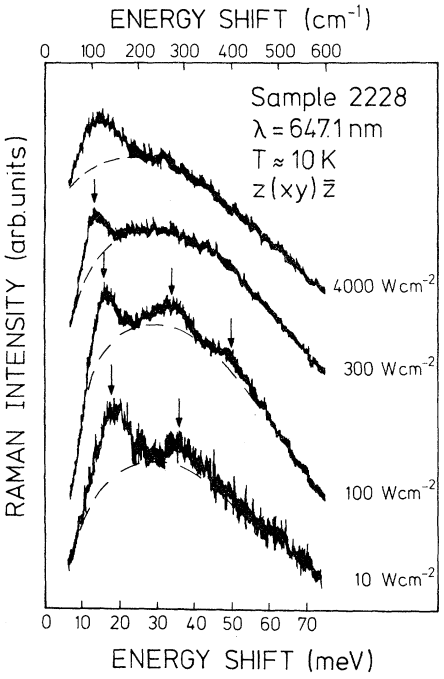

FIG. 6. Single-particle spectra at different excitation intensities for sample 2228.

intensity. In some cases three peaks with approximately equidistant energies are observed. These excitation lines are identified as $\Delta=1$, $\Delta=2$, and $\Delta=3$ intersubband transitions in the *n-i-p-i* layers.

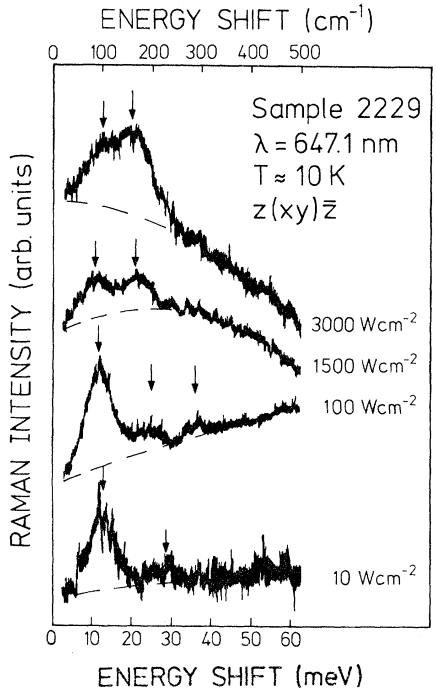

FIG. 7. Single-particle spectra at different excitation intensities for sample 2229.

In Fig. 8 the positions of the subband excitations are compared with the calculated splittings. The full points mark the experimental results. The crosses are the results of Ref. 8 obtained for sample 2228. With the use of the procedure discussed above, the two-dimensional carrier density has been derived from the luminescence experiments carried out simultaneously with the Raman measurements. The potential well is only an ideal harmonic oscillator for extremely low excitation. For higher N the subband splittings are not exactly equal. Therefore, the solid lines in Fig. 8 show the theoretical results for the average subband splittings $\Delta=1$, 2, and 3. These have been obtained by weighting the excitation energies by the number of electrons which can make the transitions. The energies calculated in this way are in excellent agreement with the experimental results for all three samples.

The arrows in Fig. 8 mark the carrier density at which the Fermi energy according to the calculations reaches the top of the potential wells in the conduction band. At higher electron concentrations part of the carriers occupy states for which the overlap of the electron wave functions between neighboring wells is strong enough to broaden the subbands into minibands with considerable dispersion perpendicular to the layers. At the same time the mean subband distance gets smaller. This is observed in the spectra at high excitation intensities. In sample 2229 (Fig. 7) the subband excita-

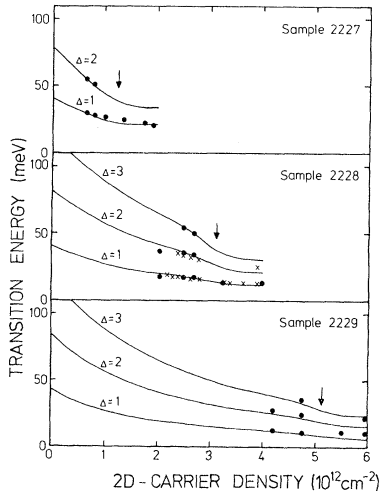

FIG. 8. Comparison of experimental subband transition energies with the results of self-consistent calculations. The dots mark our own experimental values, the crosses are from Ref. 8. For carrier densities higher than those marked by arrows the Fermi energy lies above the top of the potential wells.

tions merge at 3000 Wcm^{-2} resulting in a broad single-particle excitation band which is already very similar to the results obtained for the free-electron system in GaAs.[21] A similar broadening and change in line shape is observed for the other samples. At high-excitation intensities the photoexcited electrons in *n-i-p-i* crystals are therefore quasi-three-dimensional rather than two dimensional. This is also the reason that the luminescence line is more symmetric at high carrier concentrations.

V. CONCLUDING REMARKS

In summary, we have shown that new types of GaAs-doping superlattices definitely show the predicted properties such as tunable effective band gap and quantization of electrons in purely space-charge-induced potential wells. The experimental results obtained with three different types of compensated GaAs *n-i-p-i* crystals are in very good agreement with self-consistent subband calculations which are only based on the design parameters of the samples. In the calculation the effect of the finite miniband width of the subbands was treated more carefully. The spin-flip single-particle spectra clearly show this broadening at high-excitation intensities. The spectral line shapes change and become very similar to single-particle excitations of a three-dimensional electron gas.

We have also measured Raman spectra of collective excitations (coupled with LO-phonon modes) which, in principle, allow the quantitative determination of the effect of resonant screening in the electron system. With increasing excitation intensity, however, more and more subbands are occupied and the spectral line shapes become complicated. At very high density, again a quasi-three-dimensional coupled plasmon-LO-phonon spectrum is observed. Thus the *n-i-p-i* system makes it possible to study the effects on resonant screening concomitant with the continuous change from a two-dimensional to a thee-dimensional system. The coupled-mode frequencies have been calculated recently.[10] For a quantitative interpretation of the collective coupled-mode spectra, however, more theoretical work is necessary.

ACKNOWLEDGMENTS

We would like to thank G. H. Döhler and P. Ruden for detailed discussions concerning the theory and A. Fischer for the expert help in sample preparation. The work was supported by the Deutsche Forschungsgemeinschaft via SFB 128 and by the Bundesministerium für Forschung und Technologie of the Federal Republic of Germany.

[1]See, for example, R. Dingle, in *Festkörperprobleme, Advances in Solid State Physics,* edited by H. J. Queisser (Vieweg, Braunschweig, 1975), Vol. XV, p. 21; L. Esaki and L. L. Chang, Thin Solid Films 36, 285 (1976).

[2]L. L. Chang and L. Esaki, Surf. Sci. 98, 70 (1980).

[3]R. Dingle, H. L. Störmer, A. C. Gossard, and W. Wiegmann, Appl. Phys. Lett. 33, 665 (1978).

[4]See, for example, H. L. Störmer, J. Phys. Soc. Jpn. 49, 1013 (1980).

[5]G. H. Döhler, Phys. Status Solidi B 52, 79 (1972); 52, 533 (1972).

[6]G. H. Döhler, J. Vac. Sci. Technol. 16, 851 (1979).

[7]K. Ploog, A. Fischer, and H. Künzel, J. Electrochem. Soc. 128, 400 (1981).

[8]G. H. Döhler, H. Künzel, D. Olego, K. Ploog, P. Ruden, H. J. Stolz, and G. Abstreiter, Phys. Rev. Lett. 47, 864 (1981).

[9]G. H. Döhler and K. Ploog, Prog. Cryst. Growth Charact. 2, 145 (1979).

[10]P. Ruden and G. H. Döhler, Phys. Rev. B (in press).

[11]T. Ando and S. Mori, J. Phys. Soc. Jpn. 47, 1518 (1979).

[12]Even at room temperature the photoluminescence line remains relatively sharp [M. Ilegems, J. Appl. Phys. 48, 1278 (1977)].

[13]G. Abstreiter and K. Ploog, Phys. Rev. Lett. 42, 1308 (1979).

[14]A. Pinczuk, H. L. Störmer, R. Dingle, J. M. Worlock, W. Wiegmann, and A. C. Gossard, Solid State Commun. 32, 1001 (1979).

[15]E. Burstein, A. Pinczuk, and D. L. Mills, Surf. Sci. 98, 451 (1980).

[16]A. Pinczuk, J. Shah, A. C. Gossard, and W. Wiegmann, Phys. Rev. Lett. 46, 1341 (1981).

[17]K. M. Romanek, H. Nather, and E. O. Göbel, Solid State Commun. 39, 23 (1981).

[18]A. Pinczuk, J. Shah, and P. Wolff, Phys. Rev. Lett. 47, 1487 (1981).

[19]A. Pinczuk, J. M. Worlock, H. L. Störmer, R. Dingle,

W. Wiegmann, and A. C. Gossard, Solid State Commun. 36, 43 (1980).
[20]G. Abstreiter, Ch. Zeller, and K. Ploog, *Gallium Arsenide and Related Compounds, 1980,* edited by H. W. Thim (IOP, London, 1981), Vol. 56, p. 741.
[21]A. Pinczuk, G. Abstreiter, R. Trommer, and M. Cardona, Solid State Commun. 30, 429 (1979).